

Electrical conductivity in non-stoichiometric titanium dioxide at elevated temperatures

U. BALACHANDRAN*, N. G. EROR
Oregon Graduate Center, Beaverton, Oregon 97006, USA

The electrical conductivity of polycrystalline titanium dioxide prepared by a liquid mix technique was measured for the oxygen partial pressure range of 10^0 to 10^{-19} atm and temperature range of 850 to 1050°C. The data were found to be proportional to the $-1/6$ power of oxygen partial pressure for the oxygen pressure range 10^{-19} to 10^{-15} atm, and proportional to $P_{O_2}^{-1/4}$ for the oxygen pressure range $>10^{-15}$ atm. The region of linearity where the electrical conductivity varied as the $-1/4$ power of P_{O_2} increased as the temperature was decreased. There was evidence of p-type behaviour for $P_{O_2} > 10^{-2}$ atm in the temperature range 950 to 850°C, although the measured data were insufficient to assign a pressure dependence. Electrical conductivity minima in the $\log \sigma$ against $\log P_{O_2}$ plot moved to lower P_{O_2} as the temperature was decreased in the range 950 to 850°C. The measured oxygen pressure dependence of electrical conductivity in the lowest P_{O_2} region supports the oxygen vacancy defect model. The observed data are consistent with the presence of very small amounts of acceptor impurities. A binding energy of ~ 0.67 eV between the acceptor impurity and its compensating oxygen vacancy was also determined.

1. Introduction

Rutile (TiO_2) crystals have a wide range of interesting properties, many of which are associated with impurities and defects in the structure. Some of the most intriguing defects are those which are introduced by heating rutile specimens in a reducing atmosphere (vacuum, hydrogen, carbon monoxide, titanium powder). Rutile is an oxygen-deficit, semiconducting transition metal oxide at room temperature when equilibrated in an atmosphere of low oxygen activity, and is non-conducting at room temperature when equilibrated in an atmosphere of high oxygen activity. In the last decade, after the work of Fujishima and Honda [1], its interest as an anode material in the photolysis of water increased. Non-stoichiometric titanium dioxide has already been studied extensively, but there is no general agreement in the literature concerning its defect structure. A salient question is whether oxygen vacancies or titanium interstitials are the dominant defects [2-13]. Independent of the nature of the atomic disorder, the electrical conductivity is due to electrons resulting from the electronic disorder introduced by the oxygen non-stoichiometry. The electron is generally believed to travel in a narrow 3d band with effective mass $\sim 30 m_0$ (where m_0 is the free-electron mass); the mobility is governed by polar scattering at high temperatures and by scattering by impurities at intermediate temperatures [14, 15].

All of the reported data on the electrical conductivity (σ) in TiO_2 suggest that σ varies as $P_{O_2}^{-1/m}$, but the m values are different. Tannhauser [9], Moser *et al.*

[10] and Baumard *et al.* [16] found $m = 5$ at very high temperatures (1400 to 1500°C) which is in support of the existence of interstitial titanium, Ti_{int}^{4+} . In contrast, at lower temperatures (1100°C) Tannhauser [9] and Blumenthal *et al.* [10] found $m \approx 5.3$ for $P_{O_2} > 10^{-8}$ atm and $m \approx 4$ for $P_{O_2} < 10^{-8}$ atm, and Baumard *et al.* [16] reported $m \approx 4.8$ for $P_{O_2} < 10^{-8}$ atm. More recently, Marucco *et al.* [12] measured the electrical conductivity as a function of oxygen partial pressure in the temperature range 800 to 1100°C and found that the slope of the $\log \sigma$ against $\log P_{O_2}$ plots change from $-1/5$ to $-1/6$ and then $-1/4$ as P_{O_2} grows. They reported that for low P_{O_2} values, Ti_{int}^{4+} is the predominant defect and as P_{O_2} increases oxygen vacancies are produced at first in the doubly ionized form, $V_0^{\cdot\cdot}$, and then a progressive transition to singly ionized vacancies, V_0^{\cdot} . The electrical conductivity of rutile doped with niobium, tantalum or chromium is reported [17, 18] in the temperature range 1000 to 1350°C. In contrast to the situation for n-type TiO_2 , information concerning p-type rutile is quite limited. The first detailed study of the electron holes in rutile was that of Rudolph [19] who observed a positive thermopower in his iron-doped sintered samples. A p-n transition has been observed by Yahia [11] and Tani and Baumard [18] in acceptor-doped TiO_2 .

There are disagreements as to the extent of non-stoichiometry in rutile. From isopiestic and e.m.f. measurements Blumenthal and Whitmore [20] concluded that the homogeneity range of TiO_{2-x} at 900 to

*Present address: Argonne National Laboratory, Argonne, Illinois 60439, USA.

1000°C extends to a value of $x \sim 0.01$. However, Anderson and Khan [21] reported a value of 0.008 for x at 1000°C. Kofstad [6] indicated a value $m = 2$ for $x < 10^{-3}$ and $m = 6$ for $x > 10^{-3}$ in $x \propto P_{O_2}^{-1/m}$ for TiO_{2-x} in the temperature range 920 to 1220°C. Forland [7] suggested an m value independent of x but varying with temperature from 6.7 at 934°C to 6.0 at 1194°C. In both cases, the non-stoichiometry was interpreted on the basis of an oxygen vacancy model. The interpretation of Picard and Gerdanian [4] leads to doubly ionized oxygen vacancies, $V_O^{2\cdot}$, at small deviations from stoichiometry and to interstitial titanium at higher deviations. Both Dirstine and Ross [22] and Alcock *et al.* [23] reported $m \approx 5$ and this suggests the existence of Ti_{int}^{4+} .

The random point defect model is no longer appropriate for describing the non-stoichiometric disorder in rutile when the deviation from stoichiometry is large ($n < 10$ for Ti_nO_{2n-1}). It is now well known that the region TiO_x ($1.75 \leq x \leq 1.90$) contains a series of ordered phases Ti_nO_{2n-1} , with $4 \leq n \leq 10$ [24]. The structures of the first six of these are derived from rutile by regular crystallographic shear [24, 25].

In the present study, the high-temperature equilibrium electrical conductivity of polycrystalline TiO_2 has been measured as a function of oxygen partial pressure in the temperature range 850 to 1050°C. The change in oxygen pressure dependence of electrical conductivity has been interpreted on the basis of the presence of small amounts of acceptor impurities in the sample, and the predominant defect structures are identified by matching the observed electrical characteristics to specific defect models. The cation acceptor impurities and their compensating oxygen vacancies

TABLE I P_{O_2} dependence of electrical conductivity in the region 10^{-18} to 10^{-15} atm

T (°C)	m for $\sigma_n \propto P_{O_2}^{-1/m}$
850	5.84 ± 0.09
900	5.80 ± 0.05
950	5.93 ± 0.08
1000	5.96 ± 0.12
1050	5.70 ± 0.13

were found to form defect pairs and the binding energy of the defect complex was determined.

2. Experimental procedure

The samples used in this investigation were prepared from tetraisopropyl titanate solution (Tyzor, Dupont Co.). The powder samples obtained by heating the titanate solution were pressed into thin rectangular slabs (2.1 cm \times 0.6 cm \times 0.05 cm) under a load of 40 000 psi (276 MPa) and sintered in air at 1350°C for a period of 10 h. The density of the sintered slabs was 96% of the theoretical density. Electrical conductivity specimens were cut from this slab using a Sandblaster unit. A conventional four-probe direct current technique was employed for all electrical conductivity measurements. The experimental details have been previously described [26, 27].

3. Results and discussion

The electrical conductivity of polycrystalline titanium dioxide in the temperature range 850 to 1050°C and in equilibrium with oxygen partial pressures between 10^{-19} and 10^0 atm is shown in Fig. 1. Two distinct regions were found from the $\log \sigma$ against $\log P_{O_2}$ plot for $P_{O_2} < 10^{-2}$ atm. The slopes of the straight lines

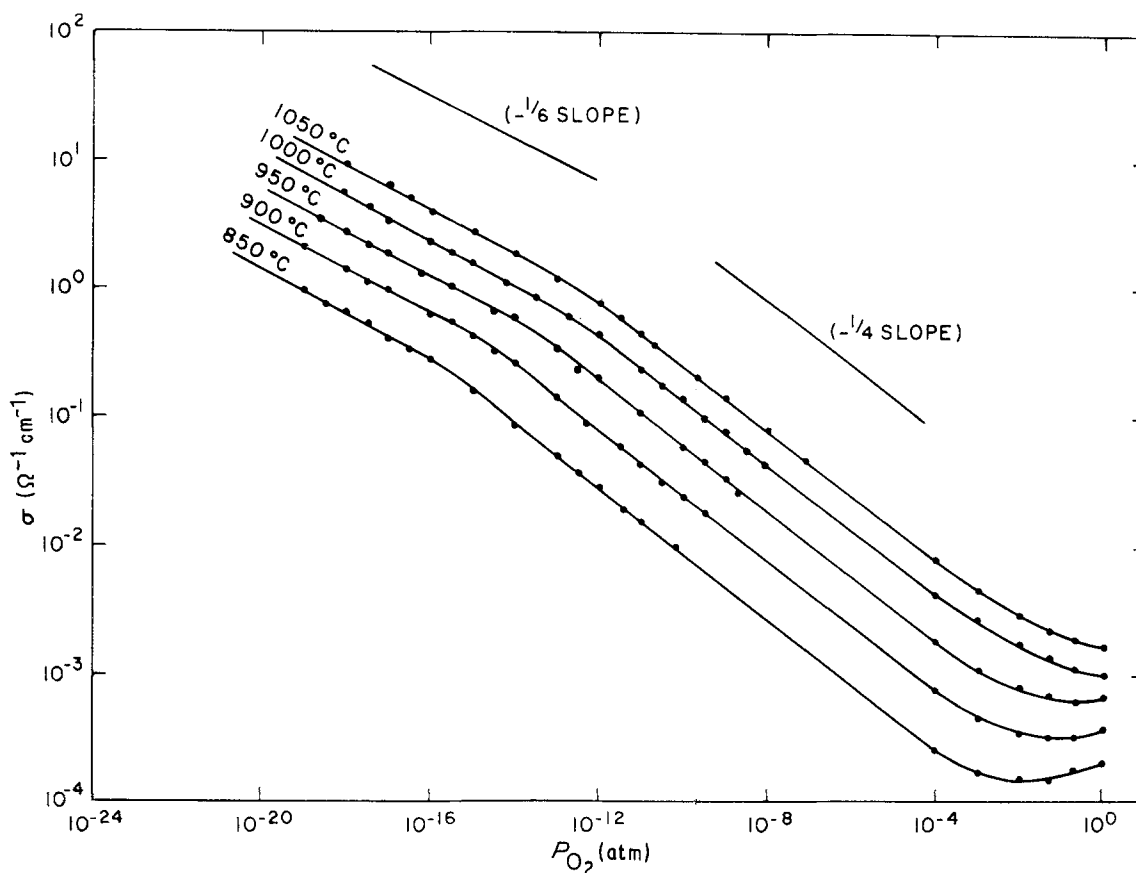


Figure 1 The electrical conductivity of polycrystalline TiO_2 as a function of oxygen partial pressure at constant temperature.

TABLE II P_{O_2} dependence of electrical conductivity in the region 10^{-14} to 10^{-4} atm

T ($^{\circ}\text{C}$)	m for $\sigma_n \propto P_{O_2}^{-1/m}$
850	3.96 ± 0.02
900	3.94 ± 0.02
950	3.94 ± 0.05
1000	4.20 ± 0.07
1050	4.25 ± 0.07

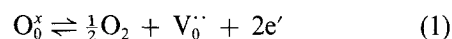
drawn through the data points are given in Tables I and II. The results show that the electrical conductivity of TiO_2 is proportional to $\approx -1/6$ power of the oxygen partial pressure for $P_{O_2} < 10^{-15}$ atm (Table I). As the P_{O_2} value is increased further, the conductivity is found to be proportional to $P_{O_2}^{-1/4}$ (Table II). The P_{O_2} value where the conductivity changes its dependence on oxygen activity depends on the equilibrium temperature. p-type conduction is observed at temperatures 850 to 950 $^{\circ}\text{C}$ and $P_{O_2} > 10^{-2}$ atm. The different regions of P_{O_2} dependence for conductivity are discussed separately in the following text.

3.1. Region I: $P_{O_2} = 10^{-19}$ to 10^{-15} atm

The $\log \sigma$ - $\log P_{O_2}$ data (Fig. 1) are linear for four decades of oxygen partial pressure for a given temperature. A slope of approximately $-1/6$ is found for the $\log \sigma$ - $\log P_{O_2}$ data (Fig. 2 and Table I). In this region of temperature and P_{O_2} , the reported results in the literature [9, 10, 16] suggest that interstitial titanium ions are the dominant defect in this non-stoichiometric oxide. The slope of $\approx -1/6$ observed in this region is similar to that found for alkaline earth titanates [26, 28-34] and in $\alpha\text{-Nb}_2\text{O}_5$ [35].

The variation of the electrical conductivity with oxygen partial pressure is calculated in terms of the oxygen vacancy defect model. The basis for the cal-

ulation is the reaction that represents the formation of a doubly ionized oxygen vacancy, $V_o^{\cdot\cdot}$, and two electrons, e' , available for conduction by the removal of an oxygen from a normal lattice site into the gas phase. The reaction is



With two electrons resulting from each oxygen vacancy, it follows that $[n]$, the concentration of electrons,

$$[n] \cong 2[V_o^{\cdot\cdot}] \quad (2)$$

The chemical mass-action expression for Equation 1 combined with Equation 2 yields the following expression for electrical conductivity, σ ;

$$\sigma = 2^{1/3} P_{O_2}^{-1/6} e \mu \exp\left(\frac{\Delta S_f}{3R}\right) \exp\left(\frac{-\Delta H_f}{3RT}\right) \quad (3)$$

where ΔH_f and ΔS_f are the enthalpy and entropy changes, respectively, associated with Equation 1, e the electronic charge, and μ the mobility of the conduction electrons. At constant temperature, assuming that the mobility is independent of the change in concentration of oxygen vacancies, a plot of the logarithm of the electrical conductivity against the logarithm of P_{O_2} should result in a straight line with a slope of $-1/6$. The data in Table I are in good agreement with the predicted $-1/6$ dependence for conductivity on the oxygen partial pressure and in support of the doubly ionized oxygen vacancy model.

An indication of the magnitude of ΔH_f , the enthalpy of the oxygen extraction reaction (Equation 1), is typically obtained from Arrhenius plots of the conductivity, as deduced from Equation 3. This procedure neglects contributions from the temperature dependences of the carrier mobility or density of states. The

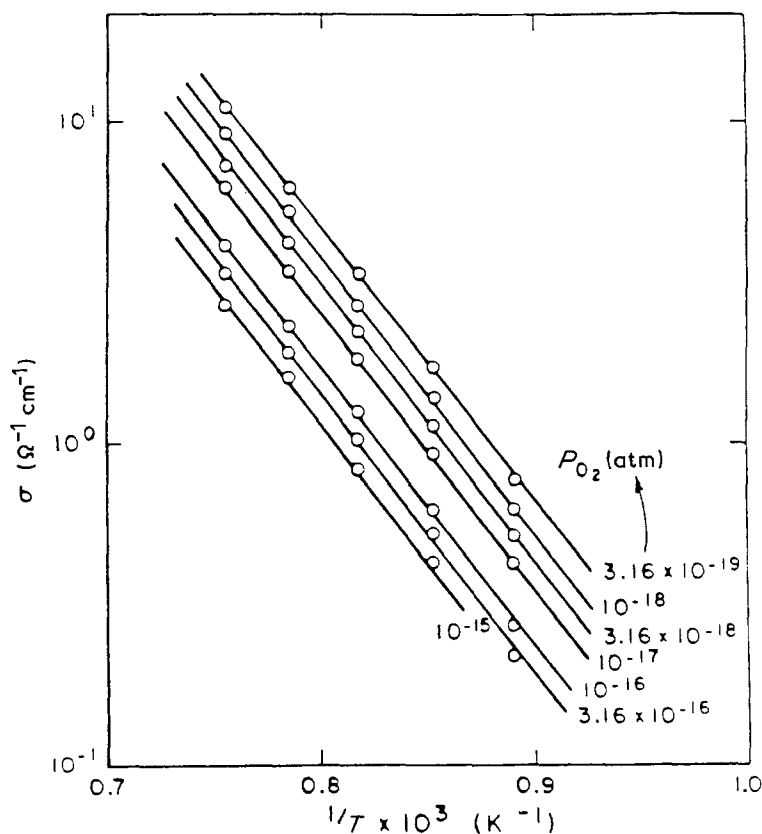


Figure 2 Temperature dependence of electrical conductivity in the P_{O_2} region 10^{-19} to 10^{-15} atm.

TABLE III Arrhenius slopes for electrical conductivity in the region 10^{-18} to 10^{-15} atm

P_{O_2} (atm)	Arrhenius slopes (kcal mol ⁻¹)*
3.16×10^{-19}	38.69 ± 0.37
10^{-18}	39.56 ± 0.36
3.16×10^{-18}	39.01 ± 0.50
10^{-17}	39.52 ± 0.41
3.16×10^{-17}	39.52 ± 0.52
10^{-16}	38.33 ± 0.49
3.16×10^{-16}	38.19 ± 0.33

* 1 kcal mol⁻¹ = 4.187 kJ mol⁻¹.

calculated slope values (in kcal mol⁻¹) from the Arrhenius plots (see Fig. 2) are given in Table III. An average value of 1.69 eV (39 kcal mol⁻¹ or 163 kJ mol⁻¹) is estimated for $\Delta H_f/3$. It should be pointed out here that ΔH_f should be three times the value given in Table III, or 5.07 eV (117 kcal mol⁻¹ or 490 kJ mol⁻¹).

3.2. Region II: $P_{O_2} = 10^{-15}$ to 10^{-2} atm

A slope of $\approx -1/4$ is found for the $\log \sigma$ - $\log P_{O_2}$ data (Fig. 3 and Table II). Most of the authors [4, 9, 13] who found $\sigma \propto P_{O_2}^{-1/4}$ attributed this relation to the existence of triply ionized titanium interstitials (Ti_{int}^{3+}). Recently, Marucco *et al.* [12] attributed the $-1/4$ dependence for conductivity on P_{O_2} to singly ionized oxygen vacancies, V_o . These interpretations presuppose that the effects of the impurities can be neglected, but this presupposition does not appear probable at near-atmospheric pressures. The low oxygen partial pressure data for non-stoichiometry in titanium dioxide has been extrapolated [36] to "atmospheric pressure" at 1100°C. This extrapolation resulted in an estimated

TABLE IV Arrhenius slopes for electrical conductivity in the region 10^{-14} to 10^{-9} atm

P_{O_2} (atm)	Arrhenius slopes (kcal mol ⁻¹)*
10^{-14}	47.12 ± 1.05
10^{-13}	46.87 ± 1.54
10^{-12}	48.66 ± 1.42
10^{-11}	49.05 ± 1.04
10^{-10}	49.45 ± 1.06
10^{-9}	49.85 ± 1.22

* 1 kcal mol⁻¹ = 4.187 kJ mol⁻¹.

native defect concentration in pure rutile of 10^{-3} at % (10 p.p.m.). Lower temperatures would result in even less native disorder. This means that extraordinary purities are required in order for the electrical properties of TiO₂ to be free from impurity effects at high oxygen activities.

The present authors [26, 32, 37] have observed an extensive range of $P_{O_2}^{-1/4}$ dependence for conductivity in the oxygen-deficient region below the p-n transition in SrTiO₃, CaTiO₃ and TiTa₂O₇ and attributed it to the presence of background acceptor impurities in the samples. Similar results were obtained by Chan and co-workers [29, 34, 38] and Inoue and Iguchi [39] in SrTiO₃ and BaTiO₃. Potential acceptor impurities are naturally much more abundant than potential donor elements. We believe that the undoped TiO₂ sample used in this investigation also contains some unknown acceptor impurities. The possible acceptor impurities are chromium, iron and aluminium on titanium sites. Considering a single-level acceptor impurity, the condition of charge neutrality will be

$$[I_m] \approx 2[V_o] \quad (4)$$

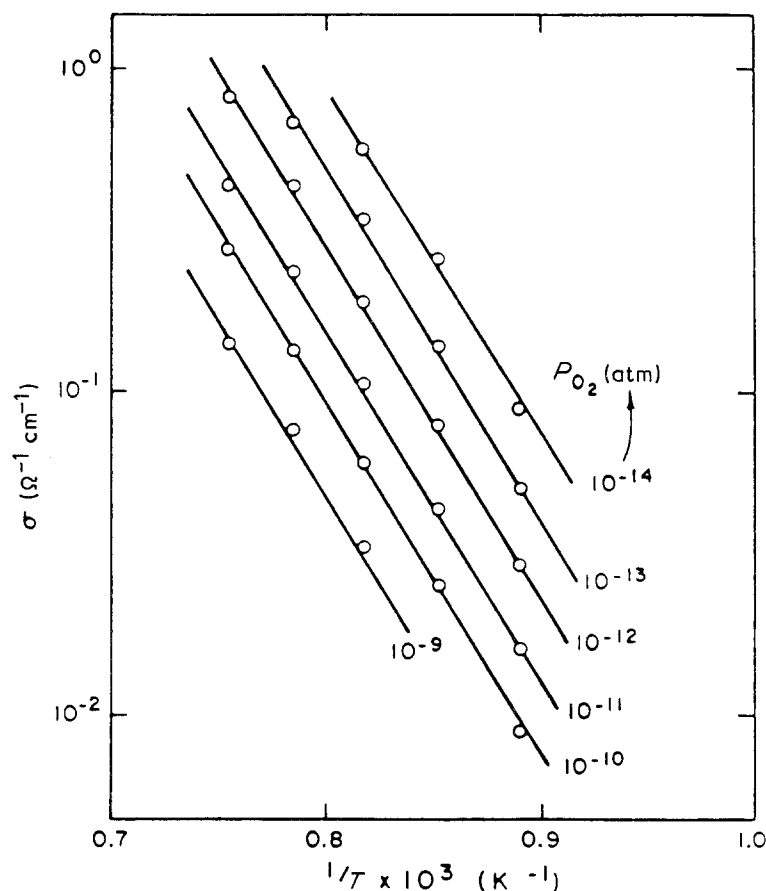


Figure 3 Temperature dependence of electrical conductivity in the P_{O_2} region 10^{-14} to 10^{-9} atm.

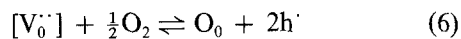
where I'_m is the singly ionized acceptor impurity, such as Al'_{Ti} . With this neutrality condition and the mass-action expression for Equation 1, the electrical conductivity varies with oxygen partial pressure as shown below:

$$\sigma = 2^{1/2} \frac{1}{[I'_m]^{1/2}} P_{O_2}^{-1/4} e\mu \exp\left(\frac{\Delta S_f}{2R}\right) \exp\left(\frac{-\Delta H_f}{2RT}\right) \quad (5)$$

The P_{O_2} dependence of conductivity in this region (listed in Table II) is in excellent agreement with the predicted value of $-1/4$ by the above impurity model. The values of $\Delta H_f/2$ derived from the Arrhenius slopes (see Fig. 3) are shown in Table IV. An average value of 2.12 eV (49 kcal mol⁻¹ or 205 kJ mol⁻¹) is estimated for $\Delta H_f/2$ in this region.

3.3. p-type region

The measured electrical conductivities in the P_{O_2} region $> 10^{-2}$ atm and in the temperature range 950 to 850°C indicate p-type behaviour or oxygen-excess conductivity. The observed data are not sufficient to assign an oxygen pressure dependence for the p-type conductivity. The P_{O_2} value where the p-n transition occurs moves to lower P_{O_2} as the temperature is decreased from 950 to 850°C. It was shown in the perovskite oxides [26, 28-30, 32, 34, 38] that the p-type conductivity arises from the incorporation of oxygen into the impurity-related oxygen vacancies where the reaction is



where $[p] \equiv h^{\cdot}$. The condition of charge neutrality in this region is the same as that observed in Region II,

$$[I'_m] \approx 2[V_0^{\cdot\cdot}] \quad (4)$$

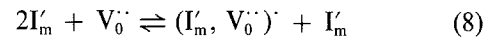
The chemical mass-action expression for Equation 6

combined with Equation 4 gives

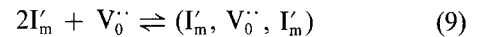
$$\sigma \propto P_{O_2}^{1/4} \quad (7)$$

The $+1/4$ dependence for conductivity on P_{O_2} will be observed only if the acceptor content is large enough to move the p-n transition to lower P_{O_2} values ($\approx 10^{-5}$ atm). The $+1/4$ slope in the $\log \sigma$ - $\log P_{O_2}$ plots have been observed in alkaline-earth titanates [26, 28-30, 32, 34, 38] in the P_{O_2} region greater than 10^{-5} atm. For the present sample, p-type conductivity at temperatures above 950°C could be observed at oxygen partial pressures much greater than 1 atm. The band gap determined from the limited minima data in the conductivity (3.07 eV) is consistent with the published values (3.0 to 3.2 eV) [17, 39].

The background acceptor impurity concentration in the undoped sample was estimated from the electrical conductivity value at the boundary between the impurity-insensitive and impurity-controlled regions, i.e. the break-point between $-1/6$ and $-1/4$ slope in the $\log \sigma$ - $\log P_{O_2}$ plots. The derived apparent net acceptor concentration from each conductivity isotherm is plotted in Fig. 4. There is a decrease in apparent acceptor content with decreasing temperature. This temperature dependence indicates that there is some degree of association between I'_m and $V_0^{\cdot\cdot}$ as shown below:



or



where $(I'_m, V_0^{\cdot\cdot})'$ and $(I'_m, V_0^{\cdot\cdot}, I'_m)$ represent charged and neutral defect complexes, respectively, with the defects electrostatically bound to adjacent lattice sites. The association expressed in Equation 8 will probably be the preferred association since trimers have been shown to be less dominant, even though they are

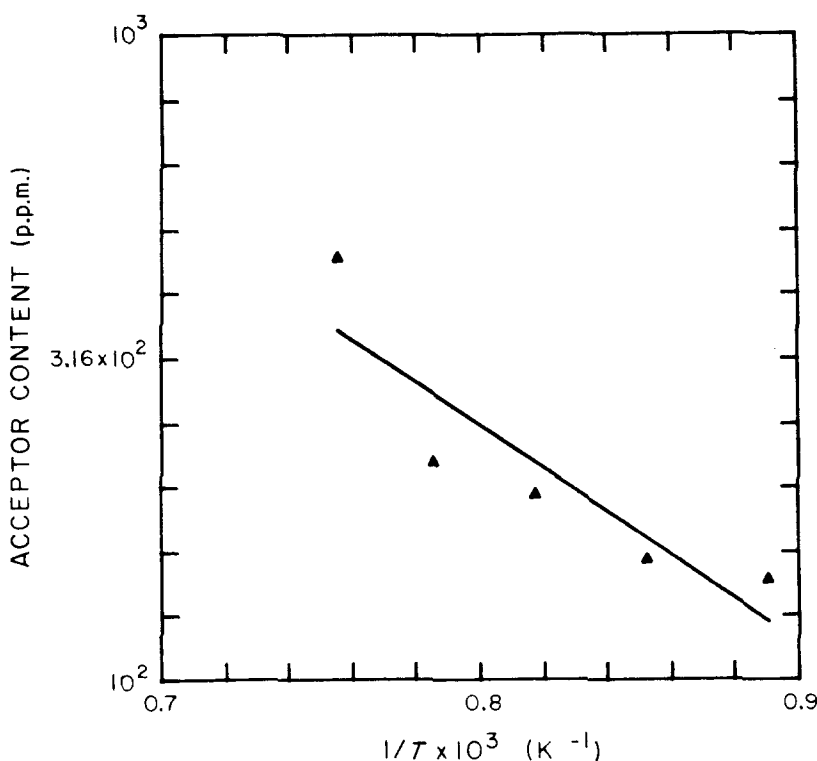
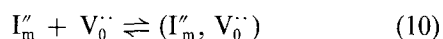


Figure 4 The net acceptor concentration of the undoped TiO_2 sample as a function of temperature, derived from conductivity data.

electrically neutral, because of entropy effects [40]. If the acceptors are doubly ionized, I_m'' , they may associate with the doubly ionized oxygen vacancies to form neutral vacancy pairs as shown below:



The association of acceptor impurities with the corresponding oxygen vacancies that were created to preserve charge neutrality (Equation 4) can be tested by measuring the oxygen chemical diffusion coefficient as a function of acceptor-dopant concentration. Free oxygen vacancies will enhance the oxygen diffusion coefficient, while those oxygen vacancies that are bound to the acceptor impurities will be less effective.

A value of 0.67 ± 0.15 eV is obtained for the enthalpy of association, ΔH_a , from the Arrhenius plots of the conductivity at the boundary between the impurity-insensitive and impurity-controlled regions. This value is not an unrealistic magnitude for the charged defects such as I_m' and V_0'' on adjacent lattice sites, when it is recalled that the association enthalpies for trivalent impurity cations and cation vacancies in alkali halides are in excess of 1 eV, which is close to the Coulombic energy [41]. The degree of association can be significant to quite high temperatures even when only one of the defects is doubly ionized. It has been proposed that defect pairs of the type (M_{Ni}', V_{Ni}'') make significant contributions to the diffusion of Al^{3+} and Cr^{3+} in NiO up to nearly 1800°C [40, 42].

The impurity content of the sample used for electrical conductivity measurements, as determined by the emission spectrographic technique, is shown in Table V. It should be pointed out here that for the case of undoped BaTiO₃ prepared by the liquid mix technique from the tetraisopropyl titanate solution, Chan and Smyth [29] reported net acceptor impurities of about 130 p.p.m. The present authors [26] have estimated an accidental acceptor impurity content of 170 p.p.m. in an undoped SrTiO₃ sample prepared by the liquid mix technique. The emission spectrographic analysis is not inconsistent with these estimates.

4. Conclusions

The experimental results agree well with the predictions based on the doubly ionized oxygen vacancy defect model (Equation 1) in the P_{O_2} range 10^{-19} to 10^{-15} atm and the temperature range 850 to 1050°C.

TABLE V Impurity content of sintered TiO₂ determined by emission spectrographic technique

Element	Concentration (at p.p.m.)	Element	Concentration (at p.p.m.)
Ag	< 1	Pb	< 5
Al	< 1	Si	250
B	< 1	Sn	< 5
Cd	< 10	V	< 5
Co	< 10	Zn	< 100
Cr	< 5	Mg	50
Cu	< 1	Ca	< 10
Fe	25	Sr	< 100
Mn	1	Li	< 50
Mo	< 5	Na	< 75
Ni	< 25	K	< 1000

The logarithm of the electrical conductivity is a linear function of the logarithm of P_{O_2} at constant temperature. A slope of $-1/6$ is observed in this region. The P_{O_2} region in which the doubly ionized oxygen vacancies are dominant defects become narrow as the temperature is decreased.

The defect chemistry of undoped TiO₂ is dominated by accidental acceptor impurities and their related oxygen vacancies (Equation 4) for $P_{O_2} > 10^{-15}$ atm. Because of these acceptor impurities, a region in which the conductivity varies as the $-1/4$ power of oxygen partial pressure is observed. The p-type conductivity observed in the region $P_{O_2} > 10^{-2}$ atm at temperatures 850 to 950°C results from the incorporation of oxygen into the impurity-related oxygen vacancies (Equation 6). The net apparent acceptor concentration decreases with decreasing temperature (see Fig. 4), indicating some degree of association between the cation acceptor impurity and its compensating oxygen vacancy.

Acknowledgements

The authors thank the Gas Research Institute for their financial support in carrying out this investigation and Tektronix Inc. for the emission spectrographic analysis.

References

1. A. FUJISHIMA and K. HONDA, *Bull. Chem. Soc. Jpn* **24** (1971) 1148.
2. P. KOFSTAD, *J. Less-Common Metals* **13** (1967) 635.
3. L. N. SHEN, O. W. JOHNSON, W. D. OHLSEN and J. W. DeFORD, *Phys. Rev.* **B10** (1974) 1823.
4. C. PICARD and P. GERDANIAN, *J. Solid State Chem.* **14** (1975) 66.
5. P. H. ODIER, J. F. BAUMARD, D. PANIS and A. M. ANTHONY, *ibid.* **12** (1975) 324.
6. P. KOFSTAD, *J. Phys. Chem. Solids* **23** (1962) 1579.
7. K. S. FORLAND, *Acta Chem. Scand.* **18** (1964) 1267.
8. J. B. MOSER, R. N. BLUMENTHAL and D. H. WHITMORE, *J. Amer. Ceram. Soc.* **48** (7) (1965) 384.
9. D. S. TANNHAUSER, *Solid State Commun.* **1** (1963) 223.
10. R. N. BLUMENTHAL, J. COBURN, J. BAUKUS and W. M. HIRTHER, *J. Phys. Chem. Solids* **27** (1966) 643.
11. Y. YAHIA, *Phys. Rev.* **130** (1963) 1711.
12. J. F. MARUCCO, J. GAUTRON and P. LEMASSON, *J. Phys. Chem. Solids* **42** (1981) 363.
13. R. N. BLUMENTHAL, J. BAUKUS and W. M. HIRTHER, *J. Electrochem. Soc.* **114** (1967) 172.
14. F. A. GRANT, *Rev. Mod. Phys.* **31** (1959) 646.
15. R. G. BRECKENRIDGE and W. R. HOSLER, *Phys. Rev.* **91** (1953) 793.
16. J. F. BAUMARD, D. PANIS and D. RUFFIER, *Rev. Int. Hautes Temp. Refract.* **12** (1975) 321.
17. J. F. BAUMARD and E. TANI, *J. Chem. Phys.* **67** (1977) 857.
18. E. TANI and J. F. BAUMARD, *J. Solid State Chem.* **32** (1980) 105.
19. J. RUDOLPH, *Z. Naturforsch.* **14A** (1959) 727.
20. R. N. BLUMENTHAL and D. H. WHITMORE, *J. Electrochem. Soc.* **110** (1963) 92.
21. J. S. ANDERSON and A. S. KHAN, *J. Less-Common Metals* **22** (1970) 219.
22. R. T. DIRSTINE and C. J. ROSS, *Z. Metallkde* **70** (1979) 322.
23. C. B. ALCOCK, S. ZADOR and B. C. H. STEELE, in "Electromotive Force Measurements in High Temperature Systems", edited by C. B. Alcock (Institute of Mining and Metallurgy, London, 1968) p. 176.
24. S. ANDERSSON and L. JAHNBERG, *Arkiv. Kemi.* **21**

- (1963) 413.
25. J. S. ANDERSON and B. G. HYDE, *J. Phys. Chem. Solids* **28** (1967) 1393.
 26. U. BALACHANDRAN and N. G. EROR, *J. Solid State Chem.* **39** (1981) 351.
 27. *Idem*, *Mater. Res. Bull.* **17** (1982) 151.
 28. S. A. LONG and R. N. BLUMENTHAL, *J. Amer. Ceram. Soc.* **54** (11) (1971) 577.
 29. N. H. CHAN and D. M. SMYTH, *J. Electrochem. Soc.* **123** (10) (1976) 1585.
 30. N. G. EROR and D. M. SMYTH, *J. Solid State Chem.* **24** (3, 4) (1978) 235.
 31. L. C. WALTERS and R. E. GRACE, *J. Phys. Chem. Solids* **28** (1967) 239.
 32. U. BALACHANDRAN, B. ODEKIRK and N. G. EROR, *J. Solid State Chem.* **41** (1982) 185.
 33. W. L. GEORGE and R. E. GRACE, *J. Phys. Chem. Solids* **30** (1969) 881.
 34. N. H. CHAN, R. K. SHARMA and D. M. SMYTH, *J. Amer. Ceram. Soc.* **64** (9) (1981) 556.
 35. U. BALACHANDRAN and N. G. EROR, *J. Mater. Sci.* **17** (1982).
 36. P. KOFSTAD, "Nonstoichiometry, Diffusion and Electrical Conductivity in Binary Metal Oxides" (Wiley Interscience, New York, 1972) Chs 11-12.
 37. N. G. EROR and U. BALACHANDRAN, *J. Amer. Ceram. Soc.* **65** (9) (1982) 426.
 38. N. H. CHAN, R. K. SHARMA and D. M. SMYTH, *J. Electrochem. Soc.* **128** (12) (1981) 1762.
 39. A. INOUE and E. IGUCHI, *J. Phys. C: Solid State Phys.* **12** (1979) 5157.
 40. R. A. PERKINS and R. A. RAPP, *Met. Trans.* **4** (1973) 193.
 41. F. BENIENE and R. ROKBANI, *J. Phys. Chem. Solids* **36** (1975) 1151.
 42. W. J. MINFORD and V. S. STUBICAN, *J. Amer. Ceram. Soc.* **57** [8] (1974) 363.

*Received 21 July
and accepted 23 October 1987*